Applied Radiation and Isotopes 191 (2023) 110568

Contents lists available at ScienceDirect

Applied Radiation and Isotopes

journal homepage: www.elsevier.com/locate/apradiso

A study for gamma-ray attenuation performances of barite filled polymer composites

Mehmet Fatih Turhan [a], Ferdi Akman [b,c,*], Mustafa Recep Kaçal [d], Hasan Polat [e], İskender Demirkol [f]

[a] Afyonkarahisar Health Sciences University, Atatürk Vocational School of Health Service, Department of Medical Imaging Techniques, 03200, Afyonkarahisar, Turkey
[b] Bingöl University, Vocational School of Social Sciences, Department of Property Protection and Security, Program of Occupational Health and Safety, 12000, Bingöl, Turkey
[c] Bingöl University, Central Laboratory Application and Research Center, 12000, Bingöl, Turkey
[d] Giresun University, Arts and Sciences Faculty, Department of Physics, 28100, Giresun, Turkey
[e] Bingöl University, Vocational School Fo Technical Sciences, Department of Architecture and Urban Planning, 12000, Bingöl, Turkey
[f] Bingöl University, Faculty of Arts and Science, Department of Physics, 12000, Bingöl, Turkey

ARTICLE INFO

Keywords:
Barite
Polymer composite
Attenuation coefficient
Value layer
Build-up factor

ABSTRACT

In this study, radiation protection efficiency (*RPE*) for the coded as UP-Ba0, UP-Ba25, UP-Ba50, UP-Ba75 and UP-Ba100 at different sample thicknesses, total mass attenuation coefficient (μ/ρ), linear attenuation coefficients (μ), half value layers (*HVL*), tenth value layers (*TVL*), mean free paths (*MFP*), effective atomic numbers (Z_{eff}) and effective electron densities (N_E) were determined at various gamma energies between 59.5 and 1408.0 keV. With the help of the geometric progression (*G-P*) fitting method, the energy absorption build-up factor (*EABF*) and exposure build-up factor (*EBF*) values were calculated in the energy range from 0.015 MeV to 15 MeV for the produced composites. HPGe detector and eight radioactive sources (^{241}Am, ^{152}Eu, ^{137}Cs, ^{133}Ba, ^{60}Co, ^{57}Co, ^{54}Mn and ^{22}Na) were utilized in the experiment. Experimental results were compared with theoretical calculations and it has been observed that there is a good agreement between theoretical and experimental results. It was observed that *RPE*, μ/ρ, μ, Z_{eff} and N_E parameters increased with increasing barite amount and decreased with increasing energy, while the opposite situation was observed in *HVL*, *TVL* and *MFP* parameters. *EABF* and *EBF* values increase with increasing penetration depth. As a result, UP-Ba100 is a good radiation absorber according to the other studied barite filled polymer composites.

1. Introduction

With the development in material science in recent years, researches on different properties of the produced materials have accelerated. Some of these researches are related to the photon-material interaction studies. Accurate determination of the attenuation parameters of material is very important in terms of determining the potential usage areas of the material. In recent years, many studies exist on the attenuation parameters of the different materials and one of the is alloys (Manjunatha et al., 2019; Reda and El-Daly 2020; Aksoy 2021; Alzahran et al., 2021; Sathish et al., 2021; Mhareb et al., 2021). X-ray, gamma and neutron shielding parameters for some selected aluminum silicon alloys were investigated by Manjunatha et al. (2019). Aksoy (2021) measured fluorescence parameters such as K-shell production cross-sections and the intensity ratios as well as attenuation parameters like μ/ρ, μ, *HVL*, *TVL*, *MFP* and Z_{eff} for silver filled superconducting alloys. Sathish et al. (2021) determined the different shielding properties for some lead based binary/ternary/quaternary alloys. Different shielding property studies in glasses are increasingly ongoing because they are potential alternative absorbent materials (Aşkın et al., 2019; Abouhaswa and Kavaz 2020; Al-Hadeethia and Sayyed 2020; Lakshminarayana et al., 2021; Kurtuluş et al., 2021; Saudi and Abd-Allah 2021; Sadeq et al., 2022). Structural, physical and radiation attenuation properties of TeO_2–B_2O_3–Bi_2O_3–LiF–$SrCl_2$ and tungsten filled zinc borate and glass systems were determined by Al-Hadeethi and Sayyed (2020) and Saudi and Abd-Allah (2021). Lakshminarayana et al. (2021) investigated the μ,

* Corresponding author. Bingöl University, Vocational School of Social Sciences, Department of Property protection and Security, program of Occupational Health and Safety, 12000, Bingöl, Turkey.
E-mail address: fakman@bingol.edu.tr (F. Akman).

https://doi.org/10.1016/j.apradiso.2022.110568
Received 10 August 2022; Received in revised form 1 November 2022; Accepted 15 November 2022
Available online 21 November 2022

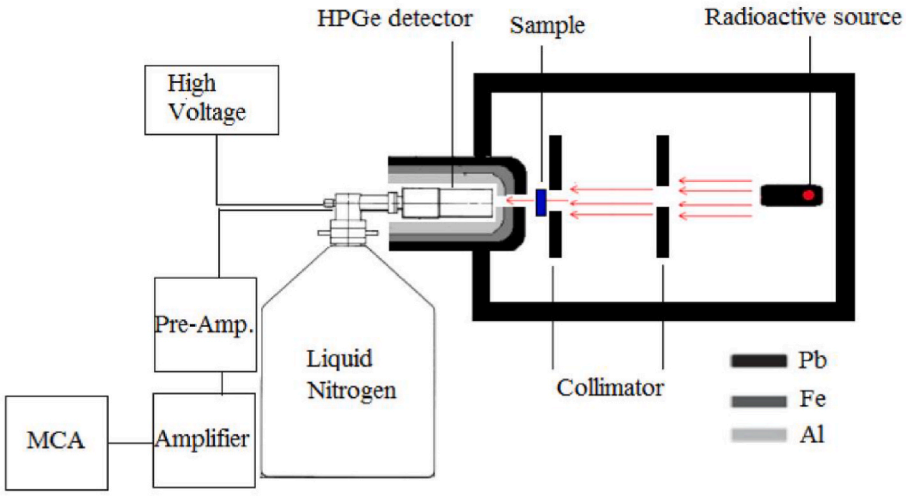

Fig. 1. The experimental arrangement.

Table 1
The percent elemental composition for the produced composites.

Sample Code	Percent Elemental Composition						ρ (g/cm^3)
	H	C	O	S	Co	Ba	
UP-Ba0	4.5946	59.9204	35.4561	–	0.0289	–	1.196
UP-Ba25	3.7030	48.2929	33.8969	2.6660	0.0233	11.4179	1.302
UP-Ba50	3.1012	40.4447	32.8444	4.4655	0.0195	19.1247	1.453
UP-Ba75	2.6677	34.7907	32.0863	5.7619	0.0168	24.6767	1.596
UP-Ba100	2.3405	30.5237	31.5141	6.7402	0.0147	28.8668	1.765

μ/ρ, Z_{eff}, N_E, *HVL*, *TVL*, *MFP* and *RPE* for bismuth lead borate glasses. Considering the risks posed by the use of lead or lead-based compounds in radiation safety, studies on radiation shielding parameters of composites (Alsayed et al., 2020; Aldhuhaibat et al., 2021; Zakaly et al., 2021; Akman et al., 2022) and ceramics (Kacal et al., 2018; Oto et al., 2019; Mhareb et al., 2020; Hannachi et al., 2022) have gained great importance. Aldhuhaibat et al. (2021) investigated the mass attenuation coefficient, mean atomic number, effective atomic cross-section, effective atomic number, electron number in the energy range from 0.662 MeV to 1.333 MeV for some selected epoxy composites. Radiation attenuation parameters were investigated for a novel polymer composite filled with niobium element by Akman et al. (2022). μ, μ/ρ, Z_{eff}, N_E, *HVL*, *TVL*, *MFP*, *EBF* and ΣR (Fast Neutron Removal Cross Section) were evaluated for some ceramics by Kacal et al. (2018). Mhareb et al. (2020) determined the structural and photon attenuation properties of $BaTiO_3$ ceramic with changed amounts of Bi and Y. In addition to the materials mentioned above, there are many studies related to attenuation parameters for various compounds (Sathiyaraj et al., 2017; Abbasova et al., 2019; Kaçal et al., 2019; Nagaraja et al., 2020; Tekin et al., 2020; ALMisned et al., 2021; Akhdar et al., 2022) in the literature. Abbasova et al. (2019) investigated the mass attenuation coefficient, effective atomic number, effective electron density, atomic cross section and electronic cross section values for the composite filler, zirconium and acrylic coating materials used in dental treatment in the energy range from 0.122 MeV to 1.408 MeV μ, μ/ρ, Z_{eff}, N_E, *HVL*, *TVL*, *EBF* and Γ (specific gamma ray constant) for $C_6H_{11}NO$, C_3H_3N, $C_2H_2Cl_2$, C_6H_4NH, $C_{10}H_8O_4$, C_6H_4S, C_4H_3N, C_2F_4, C_2H_6OSi, CH_4SiO, H_3SiN, C_2H_6Si, $C_{12}H_{32}O_8Si_8$, SiC_3H_8, $C_{44}H_{90}O_{23}$, $C_{454}H_{910}O_{228}$, $C_{908}H_{1818}O_{455}$, $C_{4540}H_{9082}O_{2271}$ and $C_{9080}H_{18162}O_{4541}$ were measured by Kaçal et al. (2019), Nagaraja et al. (2020) and Akhdar et al. (2022).

Barite is a barium-based mineral found in nature and high density and chemical inertness of this mineral make it an ideal mineral for many application areas such as drilling industry, medical industry, automobile industry, painting industry, radiation shielding area, television and computer monitors, plastic industry, etc. Barite has many different colors in nature such as yellow, brown, white, blue, gray, or even colorless. In this work, radiation shielding parameters such as *RPE* at 0.5 cm, 1.0 cm, 2.0 cm and 3.0 cm, μ/ρ, μ, *HVL*, *TVL*, *MFP*, Z_{eff} and N_E of barite filled polymer composites were experimentally determined in the different energy point from 59.5 keV to 1408.0 keV. Also *EABF* and *EBF* values for barite filled polymer composites in the energy range from 0.015 MeV to 15 MeV were calculated using G-P fitting method. Radiation attenuation parameters of the barite filled polymer composites are very limited in literature. To the best of our knowledge, radiation attenuation parameters for UP-Ba0, UP-Ba25, UP-Ba50, UP-Ba75 and UP-Ba100 have been experimentally determined for the first time in the energy number range 59.5 keV–1408 keV.

2. Materials and methods

2.1. Production of composites and experimental processes

Polyester resin was utilized as binding agent for the polymer composite preparation process. Also, we used Methyl Ethyl Ketone Peroxide (MEKP) and Cobalt Octoate (6%) as hardener and reaction accelerator, respectively. Polyester resin, MEKP and Cobalt Octoate were mixed to prepare the polymer matrix. Later, barite was added in polymer matrix as a phase material at different ratios (0, 25, 50, 75 and 100%). The ratios were determined according to unsaturated polyester by weight. Polymer composites were prepared for each percentage at 0.5, 1.0, 2.0 and 3.0 cm thicknesses.

After preparation of the barite filled polymer composite samples, gamma-ray attenuation technique was used to evaluate radiation attenuation parameters. Experiments were carried out in the energy range from 59.5 keV to 1408.0 keV. HPGe detector and different radioactive point sources (^{241}Am, ^{152}Eu, ^{137}Cs, ^{133}Ba, ^{60}Co, ^{57}Co, ^{54}Mn

Table 2
The experimental results of radiation protection efficiency at 1 cm sample thickness for the produced composites.

Energy (keV)	Radiation Protection Efficiency (%)				
	UP-Ba0	UP-Ba25	UP-Ba50	UP-Ba75	UP-Ba100
59.5	21.19 ± 0.09	80.33 ± 0.75	93.06 ± 2.11	97.35 ± 3.81	99.31 ± 3.66
81.0	19.70 ± 0.09	56.48 ± 0.32	72.59 ± 0.77	81.46 ± 0.70	90.19 ± 1.16
122.1	17.28 ± 0.14	32.73 ± 0.31	41.24 ± 0.51	49.77 ± 0.59	59.69 ± 0.84
136.5	17.37 ± 0.76	30.711.23	37.60 ± 1.52	43.49 ± 1.93	51.90 ± 2.09
276.4	13.74 ± 0.42	16.02 ± 0.49	17.82 ± 0.55	21.04 ± 0.56	25.09 ± 0.67
302.9	13.43 ± 0.19	15.32 ± 0.22	16.53 ± 0.24	18.62 ± 0.25	22.82 ± 0.31
356.0	13.29 ± 0.07	14.36 ± 0.08	14.96 ± 0.08	16.74 ± 0.10	19.71 ± 0.11
383.9	11.90 ± 0.31	13.78 ± 0.34	14.91 ± 0.42	16.76 ± 0.40	18.99 ± 0.50
511.0	10.73 ± 0.05	12.32 ± 0.06	12.39 ± 0.06	13.74 ± 0.06	16.01 ± 0.08
661.7	10.13 ± 0.05	11.39 ± 0.05	11.08 ± 0.05	12.09 ± 0.06	14.90 ± 0.07
778.9	9.59 ± 0.16	10.12 ± 0.17	10.09 ± 0.17	10.82 ± 0.18	12.60 ± 0.22
834.8	9.03 ± 0.14	9.50 ± 0.15	10.19 ± 0.16	10.95 ± 0.16	13.14 ± 0.21
867.4	8.98 ± 0.30	9.42 ± 0.35	10.18 ± 0.34	10.88 ± 0.36	12.30 ± 0.40
964.1	8.47 ± 0.08	9.13 ± 0.09	9.08 ± 0.09	9.71 ± 0.09	11.66 ± 0.11
1085.9	8.06 ± 0.13	8.73 ± 0.14	8.67 ± 0.12	9.69 ± 0.16	11.18 ± 0.19
1112.1	7.77 ± 0.06	8.47 ± 0.07	8.53 ± 0.07	9.09 ± 0.07	10.63 ± 0.08
1173.2	7.82 ± 0.05	7.99 ± 0.05	8.12 ± 0.06	9.58 ± 0.07	10.88 ± 0.07
1212.9	7.92 ± 0.35	8.34 ± 0.38	8.42 ± 0.38	9.40 ± 0.44	10.11 ± 0.47
1274.5	7.31 ± 0.04	8.01 ± 0.05	8.27 ± 0.05	8.49 ± 0.05	10.75 ± 0.06
1299.1	7.41 ± 0.25	7.92 ± 0.26	7.87 ± 0.26	8.59 ± 0.26	10.34 ± 0.35
1332.5	7.40 ± 0.04	8.15 ± 0.05	8.11 ± 0.05	8.80 ± 0.05	10.45 ± 0.06
1408.0	7.11 ± 0.03	7.37 ± 0.03	7.61 ± 0.03	8.69 ± 0.04	9.90 ± 0.05

and ^{22}Na) were utilized in the experiment as shown in Fig. 1. Crystal width and active crystal diameter of the HPGe detector were 25 mm and 70 mm, respectively. Also, the resolutions of the HPGe are 1800 eV, 585 eV and 380 eV at 1.33 MeV, 122 keV and 5.9 keV, respectively. The photons were counted in the second region 600 s ≤ s ≤ 1000 s in order to make sure acceptable statistical accuracy. Counted photons were evaluated Microcal Origin 7.5 demo version software program.

2.2. Data analysis procedure

2.2.1. Calculation of RPE, μ/ρ, HVL, TVL, MFP, Z_{eff} and N_E

One of the radiation shielding parameters is *RPE* and can be computed as follow (Sathish et al., 2021);

$$RPE(\%) = \left(1 - \frac{I}{I_0}\right) x100 \tag{1}$$

Mass attenuation coefficients can be obtained using with and without absorber counts;

$$\frac{\mu}{\rho} = \frac{1}{\rho x} \ln\left(\frac{I_0}{I}\right) \tag{2}$$

where, I_0 and I are the photon intensity without and with absorber counted by the HPGe detector, respectively. ρ and t represent the material density and absorber thickness, respectively. Elemental compositions and densities for barite filled polymer composites are listed in Table 1. The mass attenuation coefficient for each mixture or compound is evaluated as follow (Aldhuhaibat et al., 2021; Saudi and Abd-Allah, 2021);

$$\left(\frac{\mu}{\rho}\right)_{Comp} = \sum W_i \left(\frac{\mu}{\rho}\right)_i \tag{3}$$

where, the mass attenuation coefficient of the *ith* constituent element is represented with $(\mu/\rho)_i$ and the weight fraction is represented with W_i, which can be computed with the following equation;

$$W_i = \frac{n_i A_i}{\sum_j n_j A_j} \tag{4}$$

A_i is the atomic weight of the *ith* element and n_i imply the number of atoms of *ith* constituent element in the composite.

Mass attenuation coefficients and material densities can be used for calculation of the linear attenuation coefficients for barite filled polymer composites. Also, linear attenuation coefficients are used for determination of the half value layer ($\mu^{-1}\ln 2$), tenth value layer ($\mu^{-1}\ln 10$) and mean free path (μ^{-1}) (Manjunatha et al., 2019; Aksoy 2021; Alzahran et al., 2021).

Effective atomic number and electron density are evaluated with Eq. (5) and Eq. (6), respectively (Kurtuluş et al., 2021; Akman et al., 2022).

$$Z_{Eff} = \frac{\sum_i f_i A_i \left(\mu/\rho\right)_i}{\sum_j f_j \frac{A_j}{Z_j} \left(\mu/\rho\right)_j} \tag{5}$$

$$N_E = \frac{Z_{Eff.}}{A_{tot}} (N n_{tot}) \tag{6}$$

where, the fractional abundance, atomic weight, atomic number of the relative element in the composite, total atomic weight of composites and total number of atoms are with symbolized f_i, A_i, Z_j, A_{tot} and n_{tot}, respectively.

2.2.2. Calculation of build-up factors

In order to define the build-up factor, firstly equivalence atomic number (Z_{eq}) is computed and after that G-P fitting coefficients determined using the Z_{eq}. Finally, build-up factors are obtained with the help of the G-P fitting coefficients (Turhan et al., 2020; Turhan 2021).

In order to define Z_{eq}, Compton partial mass attenuation coefficient ($(\mu/\rho)_{Compton}$) and total mass attenuation coefficient ($(\mu/\rho)_{Total}$) were computed using the WinXCOM for both elements in the atomic number range from 6 to 42 and UP-Ba0, UP-Ba25, UP-Ba50, UP-Ba75 and UP-Ba100 in the energy 0.015 MeV ≤ E ≤ 15 MeV. Z_{eq} is computed by matching the ratio of $(\mu/\rho)_{Compton}$ to $(\mu/\rho)_{Total}$ of the specific energy for both composites and an element. When the ratio of $(\mu/\rho)_{Compton}$ to $(\mu/\rho)_{Total}$ lies among two consecutive ratios of elements for an composite, the interpolation of the Z_{eq} of an composite is evaluated as follow.

$$Z_{eq} = \frac{Z_1(\log R_2 - \log R) + Z_2(\log R - \log R_1)}{\log R_2 - \log R_1} \tag{7}$$

R_1, R_2 and R are the ratio for the two consecutive elements and composite at certain energy point, respectively. Z_1 and Z_2 are the atomic numbers of the concerned elements.

Geometric progression (G-P) fitting coefficients for a composite were determined by the interpolation process parallel to the equivalent atomic number determination process. G-P fitting coefficients (b, c, a, X_k and d) are evaluated using Eq. (8).

$$P = \frac{P_1(\log Z_2 - \log Z_{eq}) + P_2(\log Z_{eq} - \log Z_1)}{\log Z_2 - \log Z_1} \tag{8}$$

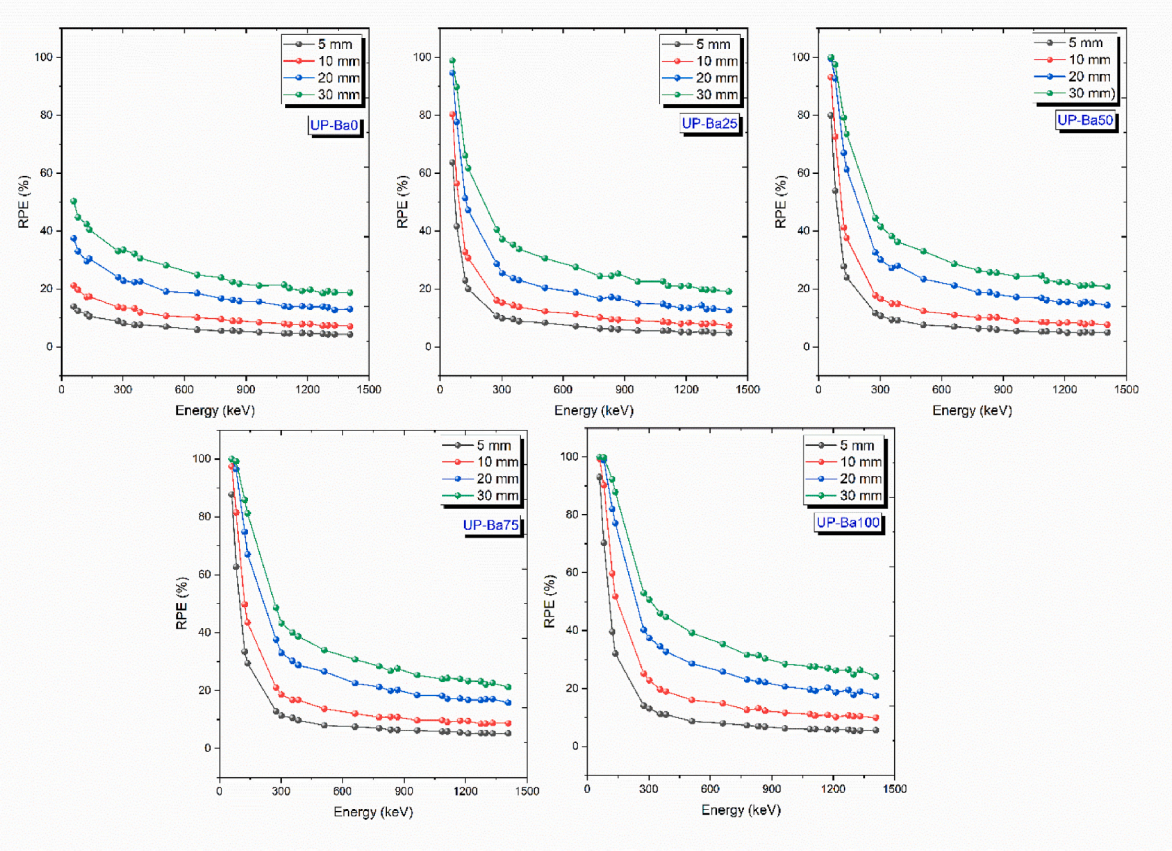

Fig. 2. RPE values for barite filled polymer composites at 0.5 cm, 1 cm, 2 cm and 3 cm thicknesses.

P_1 and P_2 are the G-P fitting coefficients of the concerned elements at certain energy point. The G-P fitting coefficients for elements were taken from the ANSI/ANS-6.4.3., 1991 standard reference database.

Finally, the energy absorption build-up factor (*EABF*) and exposure build-up factor (*EBF*) are evaluated using the G-P fitting coefficients as follow;

$$B(E,x) = 1 + \frac{b-1}{K-1}(K^x - 1) \text{for } K \neq 1 \tag{9}$$

$$B(E,x) = 1 + (b-1)x \text{for } K = 1 \tag{10}$$

where,

$$K(E,x) = cx^a + d\frac{\tanh(x/X_k - 2) - \tanh(-2)}{1 - \tanh(-2)} \text{for } x \leq 40\ mfp \tag{11}$$

E and x represent the incident photon energy and the penetration depth in *mfp*, respectively. G-P fitting coefficients are represented with b, c, a, X_k and d. b represents the value of build-up factor at 1 *mfp*.

3. Result and discussion

Radiation protection efficiencies of the barite filled polymer composite samples were determined with eq. (1) using the photon intensities with and without absorber. RPE values for the UP-Ba0, UP-Ba25, UP-Ba50, UP-Ba75 and UP-Ba100 in the energy region 59.5 keV ≤ E ≤ 1408.0 keV for 1 cm thickness are offered in Table 2. Different thickness at 0.5 cm, 1 cm, 2 cm and 3 cm of the RPE values are shown in Fig. 2. As seen from Table 2 and Fig. 2, RPE values of UP-Ba0, UP-Ba25, UP-Ba50, UP-Ba75 and UP-Ba100 decrease with increasing photon energy and take the generally minimum values for each thickness at 1408.0 keV. Also, it is clearly seen from Table 2 and Fig. 2, RPE values increase with increasing barite ratio in the composites. For example, RPE values are 8.06 ± 0.13, 8.73 ± 0.14, 8.67 ± 0.12, 9.69 ± 0.16 and 11.18 ± 0.19 for UP-Ba0, UP-Ba25, UP-Ba50, UP-Ba75 and UP-Ba100 at 1 cm thickness and 1085.9 keV, respectively. It can be said that from experimental results, RPE of barite filled polymer composite materials is much better at low energies and high thicknesses.

Experimental mass attenuation coefficient (MAC) values evaluated with the help of eq. (2) in the energy region 59.5 keV ≤ E ≤ 1408.0 keV for UP-Ba0, UP-Ba25, UP-Ba50, UP-Ba75 and UP-Ba100 are tabularized in Table 3. Also, experimental mass attenuation coefficient (MAC) values for barite (50%) are demonstrated in Fig. 3 along with theoretical Pb and Fe and experimental hematite (50%) (Turhan et al., 2021) values. Theoretical values of the mass attenuation coefficients are taken from WinXCOM (Gerward et al., 2004). Also, theoretical linear attenuation coefficient (LAC) values for the barite filled polymer composites are shown in Fig. 4 as a function of the photon energy. Experimental results are in good agreement with theoretical predictions. Uncertainties for MAC values in the experiment are found to be in the range of 2.05–4.82% for UP-Ba0, 2.04–5.00% for UP-Ba25, 2.05–4.96% for UP-Ba50, 2.05–5.07% for UP-Ba75 and 2.05–5.09% for UP-Ba100. Photon intensities with absorber (0.32–3.9%), without absorber (0.28–3.1%), mass per unit area (2.00%) and systematic errors (~3.00%) were taken into account in the assessment of uncertainties. As seen from Table 3, experimental MAC values are found to be 0.0562–0.1814 cm^2g^{-1} for UP-Ba0, 0.0528–1.1198 cm^2g^{-1} for UP-Ba25, 0.0530–1.7866 cm^2g^{-1} for UP-Ba50, 0.0543–2.2227 cm^2g^{-1} for UP-Ba75 and 0.0534–2.5482 cm^2g^{-1} for UP-Ba100 in the energy range from 59.5 keV to 1408.0 keV. Also, we reminder that MAC values between 59.5 keV and 1408.0 keV agree with WinXCOM values within ≤4.88% for UP-Ba0, ≤4.79% for UP-Ba25, ≤4.45% for UP-Ba50, ≤4.85% for UP-Ba75 and ≤ 4.87% for UP-Ba100. As seen from Fig. 3, theoretical MAC values taken from WinXCOM (Gerward et al., 2004) for Pb are 0.0542 cm^2g^{-1}-5.1286 cm^2g^{-1} in the energy region 59.5 keV ≤ E ≤

Table 3
The experimental and theoretical results of the mass attenuation coefficient ($cm^2\ g^{-1}$) for the produced composites.

Energy (keV)	UP-Ba0			UP-Ba25			UP-Ba50			UP-Ba75			UP-Ba100		
	Exp.	XCOM	R. D.[a]	Exp.	XCOM	R. D.[a]	Exp.	XCOM	R. D.[a]	Exp.	XCOM	R. D.[a]	Exp.	XCOM	R. D.[a]
59.5	0.1814 ± 0.0037	0.1886	1.97	1.1198 ± 0.0247	1.1638	3.93	1.7866 ± 0.0541	1.8244	2.12	2.2227 ± 0.0978	2.2980	3.39	2.5482 ± 0.1068	2.6576	4.29
81.0	0.1671 ± 0.0034	0.1697	1.56	0.5730 ± 0.0119	0.5897	2.91	0.8667 ± 0.0196	0.8743	0.88	1.0315 ± 0.0225	1.0783	4.54	1.1886 ± 0.0282	1.2332	3.75
122.1	0.1445 ± 0.0031	0.1502	3.04	0.2730 ± 0.0061	0.2825	3.48	0.3561 ± 0.0084	0.3722	4.52	0.4214 ± 0.0098	0.4364	3.56	0.4652 ± 0.0114	0.4852	4.30
136.5	0.1453 ± 0.0070	0.1453	0	0.2527 ± 0.0113	0.2414	4.47	0.3159 ± 0.0143	0.3065	2.98	0.3493 ± 0.0170	0.3532	1.12	0.3747 ± 0.0168	0.3886	3.71
276.4	0.1126 ± 0.0041	0.1150	2.13	0.1203 ± 0.0044	0.1263	4.99	0.1314 ± 0.0049	0.1339	1.90	0.1446 ± 0.0048	0.1394	3.60	0.1479 ± 0.0049	0.1435	2.97
302.9	0.1098 ± 0.0027	0.1112	1.28	0.1145 ± 0.0028	0.1194	4.28	0.1210 ± 0.0030	0.1250	3.31	0.1261 ± 0.0030	0.1290	2.30	0.1326 ± 0.0032	0.1321	0.38
356.0	0.1086 ± 0.0023	0.1045	3.78	0.1068 ± 0.0022	0.1091	2.15	0.1085 ± 0.0023	0.1121	3.32	0.1121 ± 0.0023	0.1143	1.96	0.1124 ± 0.0023	0.1160	3.20
383.9	0.0965 ± 0.0032	0.1015	5.18	0.1021 ± 0.0032	0.1048	2.64	0.1081 ± 0.0037	0.1070	1.02	0.1123 ± 0.0035	0.1086	3.29	0.1078 ± 0.0036	0.1098	1.86
511.0	0.0865 ± 0.0018	0.0903	4.39	0.0906 ± 0.0019	0.0908	0.22	0.0886 ± 0.0018	0.0911	2.82	0.0904 ± 0.0019	0.0914	1.11	0.0893 ± 0.0018	0.0915	2.46
661.7	0.0814 ± 0.0017	0.0807	0.86	0.0833 ± 0.0017	0.0801	3.84	0.0786 ± 0.0016	0.0797	1.40	0.0789 ± 0.0016	0.0794	0.63	0.0826 ± 0.0017	0.0791	4.24
778.9	0.0768 ± 0.0020	0.0749	2.47	0.0735 ± 0.0019	0.0740	0.68	0.0713 ± 0.0019	0.0733	2.81	0.0701 ± 0.0018	0.0729	3.99	0.0690 ± 0.0018	0.0725	5.07
834.8	0.0721 ± 0.0018	0.0725	0.55	0.0687 ± 0.0018	0.0715	4.08	0.0720 ± 0.0018	0.0708	1.67	0.0710 ± 0.0018	0.0703	0.99	0.0721 ± 0.0018	0.0699	3.05
867.4	0.0717 ± 0.0028	0.0712	0.70	0.0681 ± 0.0029	0.0701	2.94	0.0719 ± 0.0028	0.0694	3.48	0.0705 ± 0.0027	0.0689	2.27	0.0672 ± 0.0026	0.0685	1.93
964.1	0.0674 ± 0.0015	0.0677	0.45	0.0659 ± 0.0015	0.0665	0.91	0.0637 ± 0.0014	0.0658	3.30	0.0625 ± 0.0014	0.0652	4.32	0.0635 ± 0.0014	0.0648	2.05
1085.9	0.0640 ± 0.0016	0.0639	0.16	0.0629 ± 0.0016	0.0627	0.32	0.0607 ± 0.0015	0.0618	1.81	0.0624 ± 0.0016	0.0612	1.92	0.0607 ± 0.0016	0.0608	0.16
1112.1	0.0616 ± 0.0013	0.0632	2.60	0.0609 ± 0.0013	0.0619	1.64	0.0597 ± 0.0013	0.0611	2.35	0.0584 ± 0.0013	0.0605	3.60	0.0575 ± 0.0012	0.0600	4.35
1173.2	0.0621 ± 0.0013	0.0615	0.97	0.0573 ± 0.0012	0.0602	5.06	0.0567 ± 0.0012	0.0594	4.76	0.0616 ± 0.0013	0.0588	4.55	0.0590 ± 0.0012	0.0583	1.19
1212.9	0.0628 ± 0.0020	0.0604	3.82	0.0600 ± 0.0030	0.0592	1.33	0.0589 ± 0.0029	0.0584	0.85	0.0604 ± 0.0031	0.0578	4.30	0.0546 ± 0.0028	0.0573	4.95
1274.5	0.0579 ± 0.0012	0.0589	.1.73	0.0575 ± 0.0012	0.0577	0.35	0.0578 ± 0.0012	0.0569	1.56	0.0543 ± 0.0011	0.0563	3.68	0.0582 ± 0.0012	0.0558	4.12
1299.1	0.0587 ± 0.0023	0.0583	0.68	0.0568 ± 0.0022	0.0571	0.53	0.0549 ± 0.0021	0.0563	2.55	0.0550 ± 0.0020	0.0557	1.27	0.0559 ± 0.0022	0.0553	1.07
1332.5	0.0585 ± 0.0012	0.0576	1.54	0.0586 ± 0.0012	0.0564	3.75	0.0566 ± 0.0012	0.0556	1.77	0.0564 ± 0.0012	0.0550	2.48	0.0565 ± 0.0012	0.0545	3.54
1408.0	0.0562 ± 0.0012	0.0560	0.36	0.0528 ± 0.0011	0.0548	3.79	0.0530 ± 0.0011	0.0540	1.89	0.0556 ± 0.0011	0.0534	3.96	0.0534 ± 0.0011	0.0530	0.75

[a] Relative Deviation (R.D.=((*μ*/*ρ*Exp.- *μ*/*ρ*XCOM)/*μ*/*ρ*Exp)x100).

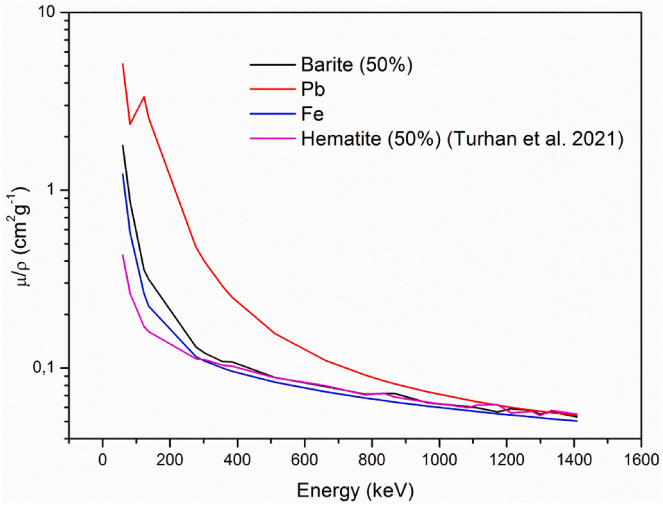

Fig. 3. Total mass attenuation coefficients of the barite (50%), Pb, Fe and hematite (50%) versus photon energy.

1408.0 keV. Also, theoretical MAC values for Fe taken from Gerward et al. (2004) are 0.0504 cm^2g^{-1}-1.2314 cm^2g^{-1} in the energy region 59.5 keV ≤ E ≤ 1408.0 keV. Experimental MAC values were founded 0.0549 cm^2g^{-1}-0.5521 cm^2g^{-1} for hematite filled polymer composites in the energy range from 59.5 keV to 1408.0 keV (Turhan et al., 2021). Experimental MAC values of barite filled polymer composites are very smaller than Pb especially low energy region. Also, experimental MAC values of barite filled polymer composites are generally larger than both Fe and hematite filled polymer composites. Additionally as seen from Fig. 4, experimental LAC values are found to be 0.0672–0.2169 cm^{-1} for UP-Ba0, 0.0687–1.4576 cm^{-1} for UP-Ba25, 0.077–2.5958 cm^{-1} for UP-Ba50, 0.0866–3.5481 cm^{-1} for UP-Ba75 and 0.0942–4.4867 cm^{-1} for UP-Ba100 in the energy range from 59.5 keV to 1408.0 keV. As seen from Table 3, Figs. 3 and 4, MAC and LAC values display the similar behaviors. While MAC and LAC values get their maximum values in the low energy region, an exponantially decrease is observed in these parameters with increasing energy and take their minimums at 1408.0 keV for all samples. According to Table 3, Figs. 3 and 4, we can say that MAC and LAC values increase with increasing barite ratio in the composites.

Half value layer (*HVL*) and tenth value layer (*TVL*) are expressed as the thickness required to reduce half and nine tenth the incident photon

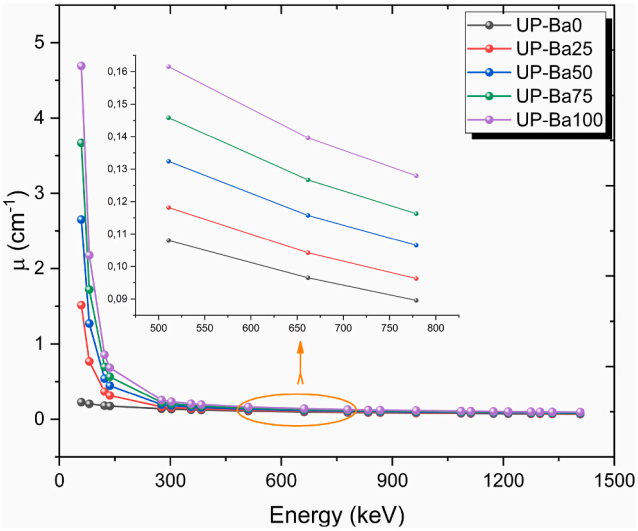

Fig. 4. The linear attenuation coefficients of the barite filled polymer composites versus photon energy.

intensity, respectively. Besides, the mean free path (*MFP*) is the average distance moved between two similar actions and these three parameters are very important parameters for studies on radiation. The experimental and theoretical results of the half value layer values are tabulated in Table 4. Also, theoretical *HVL*, *TVL* and *MFP* values are illustrated in the energy range from 59.5 keV to 1408 keV in Fig. 5. As seen from Table 4, the agreements between experimental to theoretical predictions of the *HVL* are ≤6.0% for the produced composites. As seen from Fig. 5, *TVL* values are found to be 10.61–10.25 cm, 1.58–33.53 cm, 0.89–29.92 cm, 0.65–25.92 cm and 0.51–24.44 cm in the energy range from 59.5 keV to 1408.0 keV for UP-Ba0, UP-Ba25, UP-Ba50, UP-Ba75 and UP-Ba100, respectively. Additionally, *MFP* values are determined in the length range 4.61 cm ≤ *MFP* ≤ 14.87 cm for UP-Ba0, 0.69 cm ≤ *MFP* ≤ 14.56 cm for UP-Ba25, 0.38 cm ≤ *MFP* ≤ 12.99 cm for UP-Ba50, 0.28 cm ≤ *MFP* ≤ 11.26 cm for UP-Ba75 and 0.22 cm ≤ *MFP* ≤ 10.62 cm for UP-Ba100. As seen from Table 4 and Fig. 5, *HVL*, *TVL* and *MFP* parameters increased with increasing energy and these parameters decreased with increasing barite filled ratio. Also *HVL*, *TVL* and *MFP* parameters of the UP-Ba0 are fairly higher than other barite filled polymer composites in the low energy region.

Effective atomic numbers and effective electron density of barite filled polymer composites are determined using eq. (5) and eq. (6), respectively. The theoretical effective atomic number and effective electron density results are illustrated in Figs. 6 and 7, respectively. While the effective atomic number and effective electron density values in the UP-Ba0 sample are almost constant, the change in the effective atomic number and effective electron density values with the increase of barite contribution in the UP-Ba25, UP-Ba50, UP-Ba75 and UP-Ba100 are clearly seen in Figs. 6 and 7. Z_{eff} and N_E values of the barite filled polymer composites show a similar trend. The sharply exponential decrease in effective atomic numbers and effective electron density values in the low energy region for the barite filled polymer composites indicates that the photoelectric effect is dominant in this region (from 59.5 keV to 276.4 keV). The values diminish very slightly at after 267.4 keV. After this energy point, Compton scattering effect is more dominant in the energy region 267.4 keV ≤ E ≤ 964.1 keV. After 1022 keV, the pair production is the dominant event. The photoelectric, Compton scattering and pair production cross section are proportional with energy $E^{-3.5}$, E^{-1}, E and atomic number Z^{4-5}, Z and Z^2, respectively.

Fig. 8 presents the energy absorption build-up factor (*EABF*) values against incident photon energy in the energy range of 0.015 MeV ≤ E ≤ 15 MeV at different penetration depth (0.5 *mfp*, 1 *mfp*, 5 *mfp*, 10 *mfp*, 20 *mfp* and 40 *mfp*) for UP-Ba0, UP-Ba25, UP-Ba50, UP-Ba75 and UP-Ba100. Graph of exposure build-up factor (*EBF*) values versus incident photon energy is illustrated in Fig. 9 same energies and penetration depths as Fig. 8. As can be seen from Figs. 8 and 9, UP-Ba0 is has the largest *EABF* and *EBF* values among the samples in the low and intermediate energy region. At the low energy region, where photoelectric dominates and intermediate energy region, where Compton scattering dominates, the values of *EABF and EBF* could be listed as: UP-Ba0 > UP-Ba25 > UP-Ba50 > UP-Ba75 > UP-Ba100. In the high energy region, range is reversed as: UP-Ba100 > UP-Ba75 > UP-Ba50 > UP-Ba25 > UP-Ba0. This condition can be clarified that pair production is more dominant in the high energy region and as mentioned above pair production is approximately dependent on Z^2. Also as seen from Figs. 8 and 9, *EABF* and *EBF* values increase with increasing penetration depth. For example, *EABF* values at the 0.1 MeV energy for UP-Ba25 are 1.37 for 0.5 *mfp*, 1.61 for 1 *mfp*, 2.54 for 5 *mfp*, 3.16 for 10 *mfp*, 4.15 for 20 *mfp* and 5.18 for 40 *mfp*. *EABF* and *EBF* values of the polymer composites filled with

Table 4
The experimental and theoretical results of the half value layer (cm) for the produced composites.

Energy (keV)	UP-Ba0		UP-Ba25		UP-Ba50		UP-Ba75		UP-Ba100	
	Exp.	Theo.	Exp.	Theo.	Exp.	Theo.	Exp.	Theo.	Exp.	Theo.
59.5	3.195 ± 0.065	3.072	0.476 ± 0.011	0.458	0.267 ± 0.008	0.262	0.195 ± 0.009	0.189	0.154 ± 0.006	0.148
81.0	3.468 ± 0.071	3.414	0.929 ± 0.019	0.903	0.550 ± 0.012	0.546	0.421 ± 0.009	0.403	0.330 ± 0.008	0.319
122.1	4.011 ± 0.087	3.857	1.950 ± 0.043	1.885	1.340 ± 0.031	1.282	1.030 ± 0.024	0.995	0.844 ± 0.021	0.810
136.5	3.987 ± 0.192	3.988	2.108 ± 0.094	2.206	1.510 ± 0.068	1.557	1.243 ± 0.061	1.230	1.048 ± 0.047	1.011
276.4	5.145 ± 0.187	5.039	4.428 ± 0.161	4.218	3.631 ± 0.134	3.563	3.003 ± 0.100	3.116	2.656 ± 0.088	2.737
302.9	5.276 ± 0.129	5.213	4.650 ± 0.115	4.459	3.943 ± 0.097	3.816	3.443 ± 0.082	3.366	2.961 ± 0.072	2.975
356.0	5.336 ± 0.111	5.544	4.986 ± 0.104	4.883	4.396 ± 0.091	4.255	3.873 ± 0.081	3.798	3.494 ± 0.073	3.386
383.9	6.003 ± 0.196	5.710	5.215 ± 0.165	5.082	4.413 ± 0.153	4.458	3.867 ± 0.120	3.997	3.643 ± 0.121	3.576
511.0	6.701 ± 0.137	6.417	5.880 ± 0.121	5.865	5.386 ± 0.111	5.235	4.802 ± 0.099	4.752	4.398 ± 0.091	4.291
661.7	7.120 ± 0.146	7.181	6.395 ± 0.131	6.649	6.069 ± 0.125	5.989	5.506 ± 0.113	5.471	4.755 ± 0.098	4.963
778.9	7.545 ± 0.198	7.734	7.246 ± 0.190	7.199	6.695 ± 0.176	6.507	6.194 ± 0.163	5.960	5.695 ± 0.150	5.418
834.8	8.042 ± 0.204	7.989	7.750 ± 0.198	7.449	6.627 ± 0.167	6.740	6.115 ± 0.152	6.179	5.445 ± 0.139	5.621
867.4	8.086 ± 0.316	8.136	7.819 ± 0.332	7.592	6.632 ± 0.258	6.873	6.157 ± 0.236	6.304	5.846 ± 0.223	5.736
964.1	8.593 ± 0.191	8.558	8.074 ± 0.179	8.002	7.486 ± 0.166	7.256	6.947 ± 0.154	6.661	6.186 ± 0.137	6.066
1085.9	9.048 ± 0.230	9.068	8.468 ± 0.217	8.498	7.857 ± 0.191	7.716	6.960 ± 0.182	7.092	6.471 ± 0.170	6.464
1112.1	9.407 ± 0.202	9.176	8.740 ± 0.188	8.601	7.988 ± 0.172	7.812	7.440 ± 0.160	7.181	6.827 ± 0.147	6.546
1173.2	9.337 ± 0.197	9.428	9.286 ± 0.196	8.841	8.407 ± 0.178	8.033	7.044 ± 0.149	7.386	6.661 ± 0.140	6.734
1212.9	9.223 ± 0.443	9.591	8.880 ± 0.444	8.996	8.097 ± 0.401	8.175	7.187 ± 0.365	7.517	7.198 ± 0.367	6.854
1274.5	10.017 ± 0.209	9.839	9.264 ± 0.193	9.231	8.249 ± 0.172	8.390	8.001 ± 0.167	7.716	6.745 ± 0.141	7.036
1299.1	9.879 ± 0.384	9.934	9.370 ± 0.365	9.321	8.694 ± 0.337	8.472	7.897 ± 0.287	7.792	7.026 ± 0.276	7.105
1332.5	9.899 ± 0.206	10.067	9.095 ± 0.189	9.447	8.425 ± 0.176	8.587	7.697 ± 0.160	7.898	6.954 ± 0.145	7.202
1408.0	10.310 ± 0.211	10.355	10.094 ± 0.207	9.718	9.006 ± 0.185	8.834	7.804 ± 0.160	8.125	7.358 ± 0.151	7.409

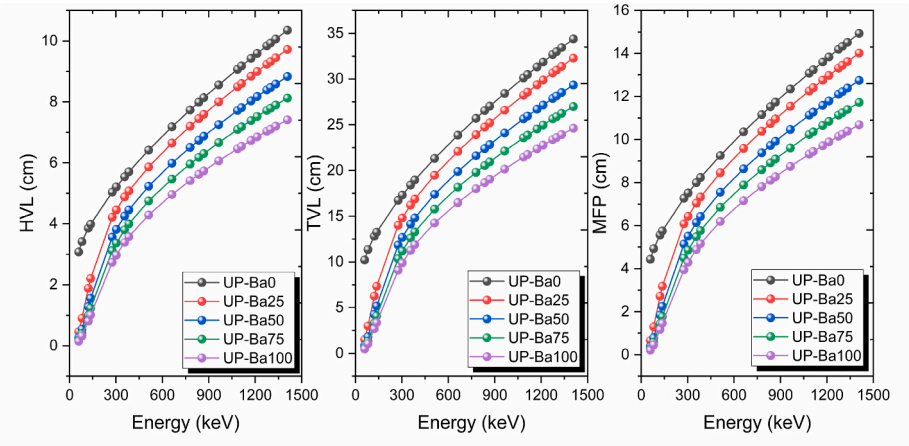

Fig. 5. *HVL*, *TVL* and *MFP* values of the barite filled polymer composites versus photon energy.

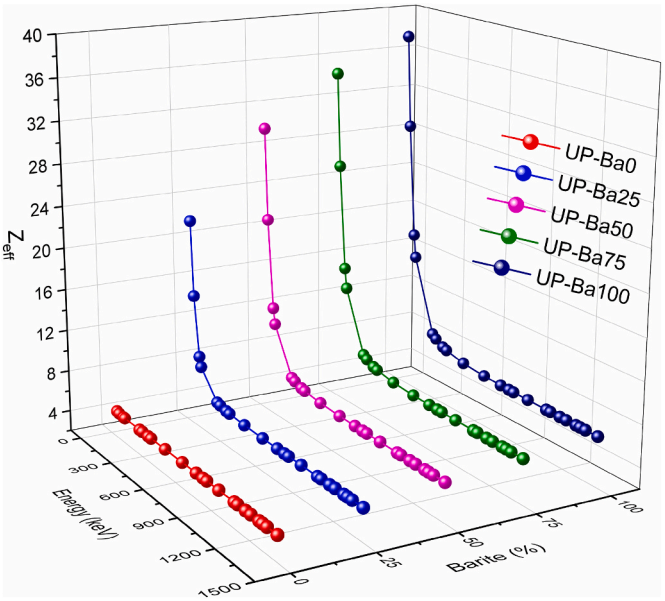

Fig. 6. Z_{eff} values against both the photon energy and filled ratio.

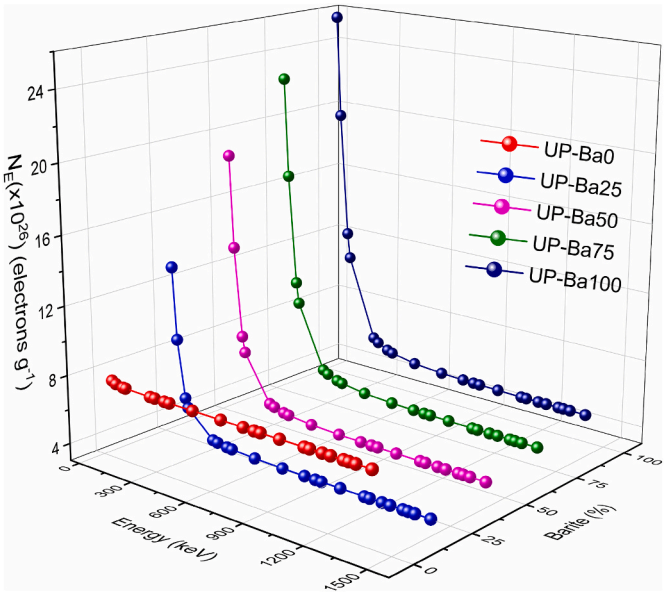

Fig. 7. N_E values against both the photon energy and filled ratio.

barite at different rates (0, 25, 50, 75 and 100%) are plotted as a function of the penetration depth at 0.015 MeV, 0.15 MeV, 1.5 MeV and 15 MeV photon energy in Figs. 10 and 11, respectively. As seen from Figs. 10 and 11, *EABF* and *EBF* values composites increase with increasing penetration depth. Also, *EABF* and *EBF* values reached their largest values at 0.15 MeV in the selected penetration range.

The gamma-ray attenuation parameters of barite filled polymer composites showed similar behavior for many other materials such as glasses (Abouhaswa and Kavaz 2020; Kurtuluş et al., 2021), alloys (Manjunatha et al., 2019; Reda and El-Daly 2020) and compounds (Kaçal et al., 2019; Turhan et. 2020; Tekin et al., 2020). It can be said that radiation attenuation parameters of UP-Ba0, UP-Ba25, UP-Ba50, UP-Ba75 and UP-Ba100 are depend on the chemical composition, density and photon energy.

4. Conclusions

In this study, *RPE* at 0.5 cm, 1.0 cm, 2.0 cm and 3.0 cm, μ/ρ, μ, *HVL*, *TVL*, *MFP*, Z_{eff} and N_E values of UP-Ba0, UP-Ba25, UP-Ba50, UP-Ba75 and UP-Ba100 were investigated in the energy region from 59.5 keV to 1408.0 keV. Also, *EABF* and *EBF* values of UP-Ba0, UP-Ba25, UP-Ba50, UP-Ba75 and UP-Ba100 were calculated in the energy range from 0.015 MeV to 15 MeV up to 40 *mfp* penetration depth. It was observed that *RPE*, μ/ρ, μ, Z_{eff} and N_E parameters increased with increasing barite amount and decreased with increasing energy, while the opposite situation was observed in *HVL*, *TVL* and *MFP* parameters. As shown in figures and tables, UP-Ba100 is a good radiation absorber among studied barite filled polymer composites. That is, it was observed that their gamma radiation attenuation capacity improved depending on the increasing amount of barite. The obtained data in this study can be used in many fields such as medical physics, health physics, radiation-related units of hospitals, nuclear physics, and space physics.

CRediT authorship contribution statement

Mehmet Fatih Turhan: Writing – review & editing, Resources, Methodology, Investigation. **Ferdi Akman:** Writing – review & editing, Supervision, Project administration, Formal analysis, Conceptualization. **Mustafa Recep Kaçal:** Validation, Resources, Methodology, Investigation. **Hasan Polat:** Methodology, Investigation. **İskender Demirkol:** Writing – original draft, Formal analysis, Data curation.

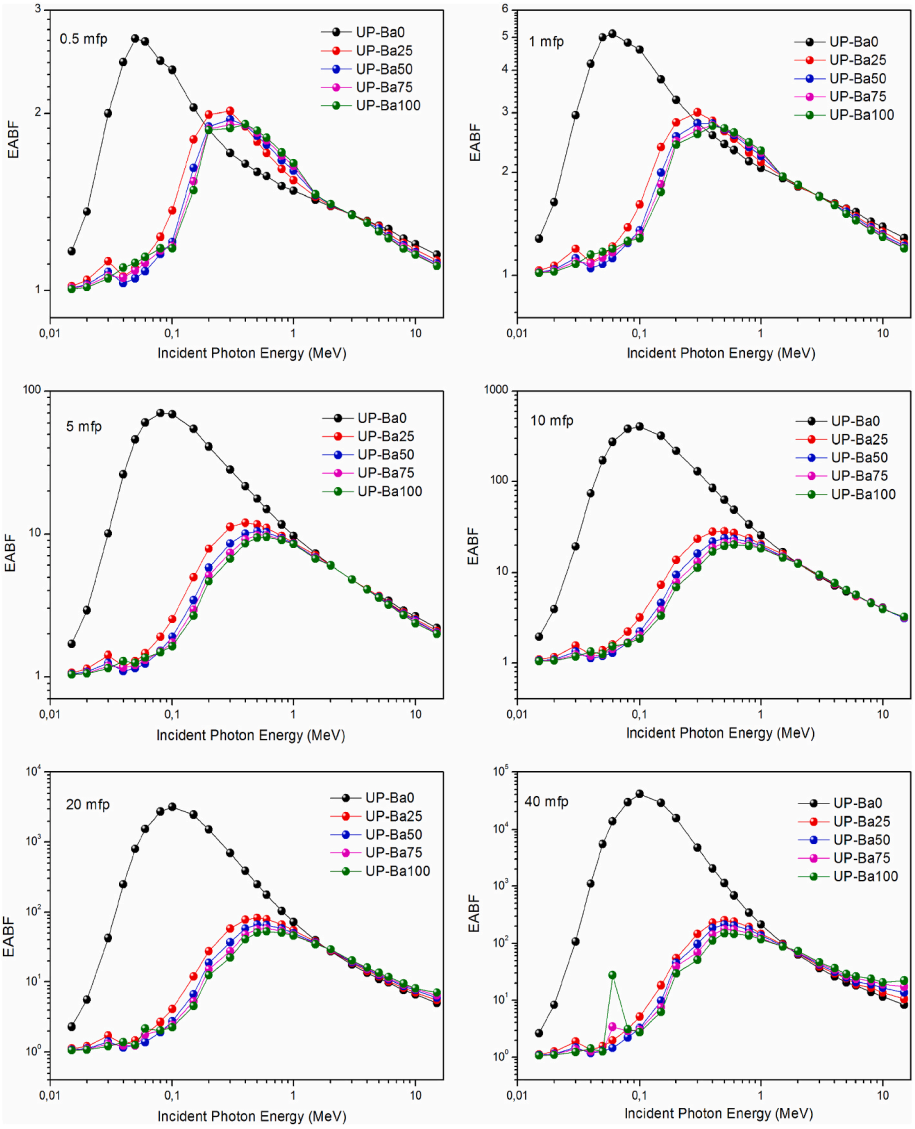

Fig. 8. *EABF* values of barite filled polymer composites in the energy region 0.015–15 MeV at 0.5, 1, 5, 10, 20 and 40 *mfp*.

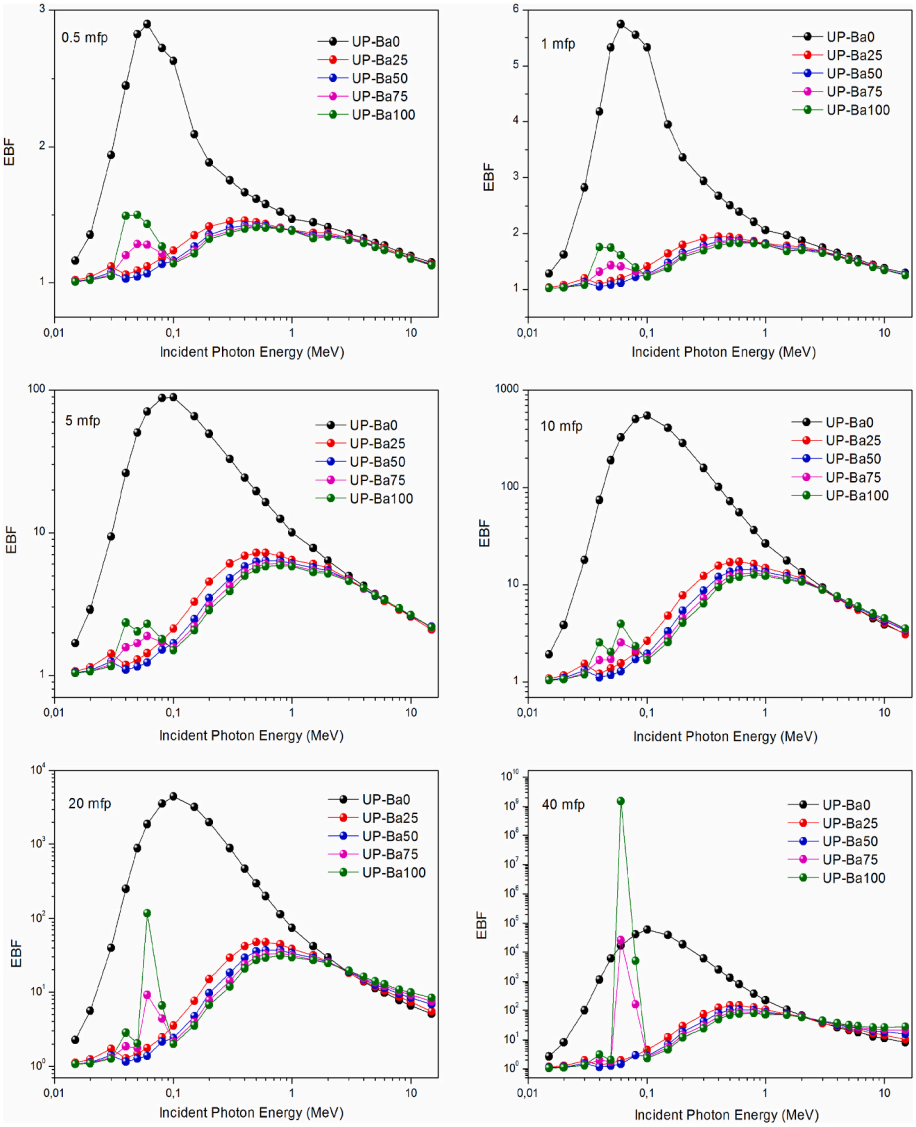

Fig. 9. *EBF* values of barite filled polymer composites in the energy region 0.015–15 MeV at 0.5, 1, 5, 10, 20 and 40 *mfp*.

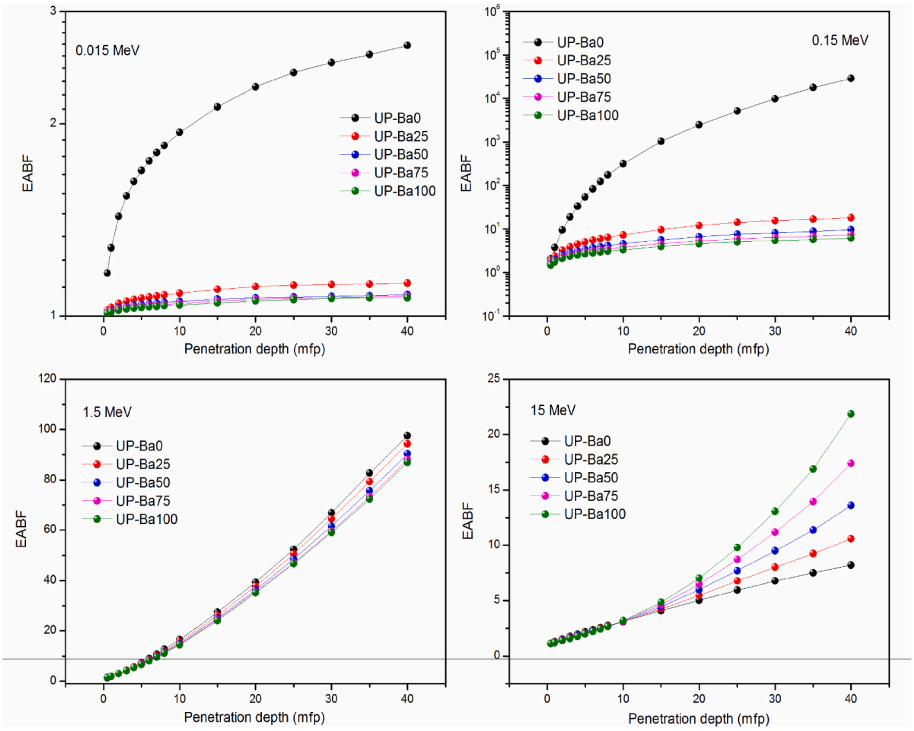

Fig. 10. *EABF* values of barite filled polymer composites up to 40 *mfp* at 0.015, 0.15, 1.5, 15 MeV.

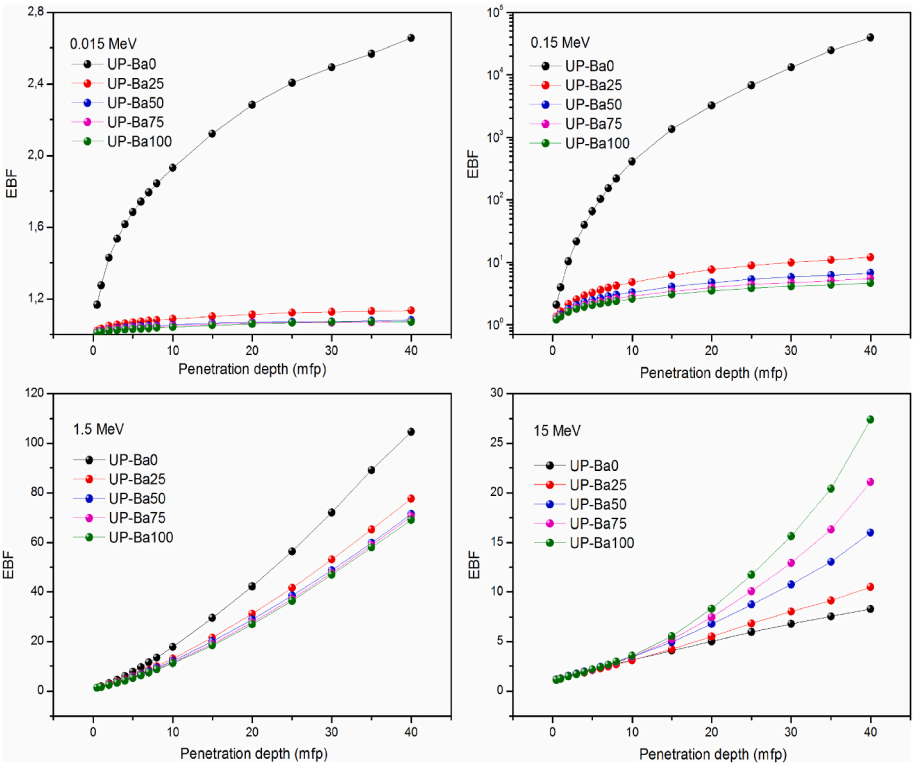

Fig. 11. *EBF* values of barite filled polymer composites up to 40 *mfp* at 0.015, 0.15, 1.5, 15 MeV.

Declaration of competing interest

The authors declare that they have no known competing financial interests or personal relationships that could have appeared to influence the work reported in this paper.

Data availability

Data will be made available on request.

Acknowledgements

The Scientific Research Projects Coordination Unit of Bingöl University supported the paper preparation process through the project with project number: BAP-TBMYO.2018.00.001.

References

Abbasova, N., Yüksel, Z., Abbasov, E., Gülbiçim, H., Tufan, M.Ç., 2019. Investigation of gamma-ray attenuation parameters of some materials used in dental applications. Results Phys. 12, 2202–2205.

Abouhaswa, A.S., Kavaz, E., 2020. Bi_2O_3 effect on physical, optical, structural and radiation safety characteristics of B_2O_3-Na_2O-ZnO-CaO glass system. J. Non-Cryst. Solids 535, 119993.

Akhdar, H., Marashdeh, M.W., AlAqeel, M., 2022. Investigation of gamma radiation shielding properties of polyethylene glycol in the energy range from 8.67 to 23.19 keV. Nucl. Eng. Technol. 54, 701–708.

Akman, F., Ogul, H., Ozkan, I., Kaçal, M.R., Agar, O., Polat, H., Dilsiz, K., 2022. Study on gamma radiation attenuation and non-ionizing shielding effectiveness of niobium-reinforced novel polymer composite. Nucl. Eng. Technol. 54, 283–292.

Aksoy, C., 2021. The X-Ray fluorescence parameters and radiation shielding efficiency of silver doped superconducting alloys. Radiat. Phys. Chem. 186, 109543.

Aldhuhaibat, M.J.R., Amana, M.S., Jubier, N.J., Salim, A.A., 2021. Improved gamma radiation shielding traits of epoxy composites: evaluation of mass attenuation coefficient, effective atomic and electron number. Radiat. Phys. Chem. 179, 109183.

Al-Hadeethi, Y., Sayyed, M.I., 2020. A comprehensive study on the effect of TeO_2 on the radiation shielding properties of TeO_2–B_2O_3–Bi_2O_3–LiF–$SrCl_2$ glass system using Phy-X/PSD software. Ceram. Int. 46, 6136–6140.

Almisned, G., Akman, F., AbuShanab, W.S., Tekin, H.O., Kaçal, M.R., Issa, S.A.M., Polat, H., Oltulu, M., Ene, A., Zakaly, H.M.H., 2021. Novel Cu/Zn reinforced polymer composites: experimental characterization for radiation protection efficiency (RPE) and shielding properties for alpha, proton, neutron, and gamma radiations. Polymers 13, 3157.

Alsayed, Z., Badawi, M.S., Awad, R., El-Khatib, A.M., Thabet, A.A., 2020. Investigation of γ-ray attenuation coefficients, effective atomic number and electron density for ZnO/HDPE composite. Phys. Scripta 95, 085301.

Alzahran, J.S., Alrowaili, Z.A., Saleh, H.H., Hammoud, A., Alomairy, S., Sriwunkum, C., Al-Buriahi, M.S., 2021. Synthesis, physical and nuclear shielding properties of novel Pb–Al alloys. Prog. Nucl. Energy 142, 103992.

ANSI/ANS-6.4.3., 1991. Gamma Ray Attenuation Coefficient and Buildup Factors for Engineering Materials. American Nuclear Society, La Grange Park, IL, USA.

Aşkın, A., Sayyed, M.I., Sharma, A., Dal, M., El-Mallawany, R., Kaçal, M.R., 2019. Investigation ofthe gamma ray shielding parameters of (100-x)[$0.5Li_2O$–$0.1B_2O_3$–$0.4P_2O_5$]-xTeO_2 glasses using Geant4 and FLUKA codes. J. Non-Cryst. Solids 521, 119489.

Gerward, L., Guilbert, N., Jensen, K.B., Levring, H., 2004. WinXCom—a program for calculating X-ray attenuation coefficients. Radiat. Phys. Chem. 71, 653–654.

Hannachi, E., Sayyed, M.I., Slimani, Y., Almessiere, M.A., Baykal, A., Elsafi, M., 2022. Synthesis, characterization, and performance assessment of new composite ceramics towards radiation shielding applications. J. Alloys Compd. 899, 163173.

Kacal, M.R., Akman, F., Sayyed, M.I., 2018. Investigation of radiation shielding properties for some ceramics. Radiochim. Acta 3030, 2018.

Kaçal, M.R., Akman, F., Sayyed, M.I., Akman, F., 2019. Evaluation of gamma-ray and neutron attenuation properties of some polymers. Nucl. Eng. Technol. 51, 818–824.

Kurtuluş, R., Kavas, T., Agar, O., Turhan, M.F., Kaçal, M.R., Dursun, I., Akman, F., 2021. Study on recycled Er-incorporated waste CRT glasses for photon and neutron shielding. Ceram. Int. 47, 26335–26349.

Lakshminarayana, G., Kumar, A., Tekin, H.O., Issa, S.A.M., Al-Buriahi, M.S., Dong, M.G., Lee, D.-E., Yoon, J., Park, P., 2021. In-depth survey of nuclear radiation attenuation efficacies for high density bismuth lead borate glass system. Results Phys. 23, 104030.

Manjunatha, H.C., Sathish, K.V., Seenappa, L., Gupta, D., Raj, A.C., 2019. A study of X-ray, gamma and neutron shielding parameters in Si- alloys. Radiat. Phys. Chem. 165, 108414.

Mhareb, M.H.A., Slimani, Y., Alajerami, Y.S., Sayyed, M.I., Lacomme, E., Almessiere, M. A., 2020. Structural and radiation shielding properties of BaTiO3 ceramic with different concentrations of Bismuth and Ytterbium. Ceram. Int. 46, 28877–28886.

Mhareb, M.H.A., Zeama, M., Elsafi, M., Alajerami, Y.S., Sayyed, M.I., Saleh, G., Hamad, R.M., Hamad, M.K.H., 2021. Radiation shielding features for various tellurium based alloys: a comparative study. J. Mater. Sci. Mater. Electron. 32, 26798–26811.

Nagaraja, N., Manjunatha, H.C., Seenappa, L., Sridhar, K.N., Ramalingam, H.B., 2020. Radiation shielding properties of silicon polymers. Radiat. Phys. Chem. 171, 108723.

Oto, B., Kavaz, E., Durak, H., Aras, A., Madak, Z., 2019. Effect of addition of molybdenum on photon and fast neutron radiation shielding properties in ceramics. Ceram. Int. 45, 23681–23689.

Reda, A.M., El-Daly, A.A., 2020. Gamma ray shielding characteristics of Sn-20Bi and Sn-20Bi-0.4Cu lead-free alloys. Prog. Nucl. Energy 123, 103304.

Sadeq, M.S., Bashter, I.I., Salem, S.M., Mansour, S.F., Saudi, H.A., Sayyed, M.I., Mostafa, A.G., 2022. Enhancing the gamma-ray attenuation parameters of mixed bismuth/barium borosilicate glasses: using an experimental method, Geant4 code and XCOM software. Prog. Nucl. Energy 145, 104124.

Sathish, K.V., Manjunatha, H.C., Vidya, Y.S., Sankarshan, B.M., Damodara Gupta, P.S., Seenappa, L., Sridhar, K.N., Alfred Cecil Raj, 2021. Investigation on shielding properties of lead based alloys. Prog. Nucl. Energy 137, 103788.

Sathiyaraj, P., Samuel, E.J.J., Valeriano, C.C.S., Kurudirek, M., 2017. Effective atomic number and buildup factor calculations for metal nano particle doped polymer gel. Vacuum 143, 138–149.

Saudi, H.A., Abd-Allah, W.M., 2021. Structural, physical and radiation attenuation properties of tungsten doped zinc borate glasses. J. Alloys Compd. 860, 158225.

Tekin, H.O., Kaçal, M.R., Issa, S.A.M., Polat, H., Susoy, G., Akman, F., Kilicoglu, O., Gillette, V.H., 2020. Sodium dodecatungstophosphate hydrate-filled polymer composites for nuclear radiation shielding. Mater. Chem. Phys. 256, 123667.

Turhan, M.F., Akman, F., Polat, H., Kaçal, M.R., Demirkol, İ., 2020. Gamma-ray attenuation behaviors of hematite doped polymer composites. Prog. Nucl. Energy 129, 103504.

Turhan, M.F., 2021. Photon interaction performance of various contrast agents: theoretical and simulation results. Appl. Radiat. Isot. 177, 109920.

Zakaly, H.M.H., Ashry, A., El-Taher, A., Abbady, A.G.E., Allam, E.A., El-Sharkawy, R.M., Mahmoud, M.E., 2021. Role of novel ternary nanocomposites polypropylene in nuclear radiation attenuation properties: in-depth simulation study. Radiat. Phys. Chem. 188, 109667.